



HAL
open science

Measurement and modelisation of dielectric properties of ferroelectrics thin layers

Raphaël Renoud, Caroline Borderon, Hartmut Wolfgang Gundel

► **To cite this version:**

Raphaël Renoud, Caroline Borderon, Hartmut Wolfgang Gundel. Measurement and modelisation of dielectric properties of ferroelectrics thin layers. ISAF 2010, Aug 2010, Edinburgh, United Kingdom. pp.1-5, 10.1109/ISAF.2010.5712244 . hal-00991546

HAL Id: hal-00991546

<https://hal.science/hal-00991546>

Submitted on 15 May 2014

HAL is a multi-disciplinary open access archive for the deposit and dissemination of scientific research documents, whether they are published or not. The documents may come from teaching and research institutions in France or abroad, or from public or private research centers.

L'archive ouverte pluridisciplinaire **HAL**, est destinée au dépôt et à la diffusion de documents scientifiques de niveau recherche, publiés ou non, émanant des établissements d'enseignement et de recherche français ou étrangers, des laboratoires publics ou privés.

Measurement and modelisation of dielectric properties of ferroelectrics thin layers

R. Renoud, C. Borderon and H.W. Gundel

IREENA, EA 1770, University of Nantes, Nantes Atlantic Universities
2 rue de la Houssinière, Nantes, F-44322, France
raphael.renoud@univ-nantes.fr

Abstract— In this study, the real and imaginary parts of the complex permittivity of PZT ferroelectric thin films are studied in the frequency range of 100 Hz – 100 MHz. The permittivity is well fitted by the Cole-Cole model. The variation of the relaxation time with temperature is described by the Arrhenius law and an activation energy of 0.38 eV is found. Due to its nonlinear character, the dielectric response of the ferroelectric sample depends on the amplitude of the applied ac electric field. The permittivity is composed of three different contributions: the first is due to intrinsic lattice, the second to domain wall vibrations and the third to domain wall jumps between pinning centers. The last one depends on the electric field so it is important to control the field amplitude to obtain the desired values of permittivity and tunability.

Dielectric permittivity, Cole-Cole approach, domain walls, temperature effects, hyperbolic law.

I. INTRODUCTION

More recently, functional ferroelectric thin films have shown a growing interest for telecommunication applications. The tunability of the dielectric constant under an applied electric field allows realizing of intelligent devices. However, the use of these materials is at present limiting because they present relatively high dielectric losses and a too low tunability. Thus a better understanding of the ferroelectric dielectric characteristics is still required.

In practical devices, the ferroelectric thin films are often used in a metal – insulator – metal geometry (MIM structure). Hence we have chosen chemical solution deposition (CSD) for an elaboration of the films on stainless steel substrates. Dielectric measurements were performed with an Agilent 4294A impedance analyzer. The relative permittivity and the losses were obtained in the 100 Hz – 100 MHz frequency range at temperatures varying from ambient temperature to 250°C. The real and the imaginary part of the permittivity were deduced and modeled using a Cole-Cole approach. The effects of temperature and of the amplitude of the ac electric field on the permittivity are studied. This allows us determination of the parameters which have a main influence on the tunability of the ferroelectric material.

II. EXPERIMENTAL PROCEDURE

The $\text{Pb}(\text{Zr}_{0.43}\text{Ti}_{0.57})\text{O}_3$ thin films (PZT 43/57) were realized by a modified sol-gel process based on the use of an alkoxide precursor. The lead acetate $\text{Pb}(\text{OOCCH}_3)_2$ is dissolved in acetic

acid CH_3COOH and the solution is heated at 100°C until complete dissolution. The solution is then cooled down at room temperature before the addition of the zirconium and the titanium n-propoxides which are mixed with a molar ratio of 43/57. Ethylene glycol $\text{HO}-\text{CH}_2-\text{CH}_2-\text{OH}$ is added in order to retain the mobility of the atoms and significantly reduces the appearance of cracks in the film [1]. Moreover, addition of ethylene glycol stabilizes the solution and prevents from precipitation [2]. Solution is then filtrated and deposited by spin coating at 4000 rpm during 20 sec on stainless steel substrates (*AISI 304*) and the samples are annealed during 2 min in a pre-heated open air furnace at 650°C. Multiple spin-coating was used when thicker PZT layers are desired.

The samples were characterized (thickness and surface of the films) by scanning electron microscopy (SEM) (*Jeol 6400*) and the crystallinity is determined by X-ray diffraction (*Siemens D5000*). The samples that crystallized in the tetragonal phase, present a polycrystalline structure with grains having an average diameter of 90 nm. The measured thickness e is 1 μm . Square gold electrodes of 0.5 mm larger (surface $S = 0.25 \text{ mm}^2$) were evaporated through a shadow mask on the films in order to form metal-ferroelectric-metal capacitors in a parallel-plate structure.

The P - E hysteresis loops (figure 1) were measured using a classic Sawyer-Tower circuit to verify the polarization state of the sample. The remanent polarization P_r is equal to $0.25 \mu\text{C}\cdot\text{cm}^{-2}$ while the value of the coercive field is $E_c = 95 \text{ kV}\cdot\text{cm}^{-1}$.

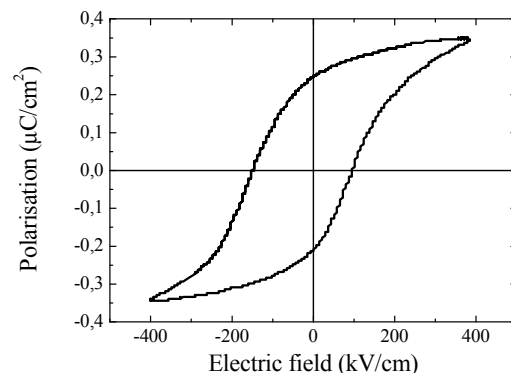


Figure 1. P - E hysteresis loops of PZT 43/57 at 300 K.

We also measure the ϵ' - E loop in order to determine the tunability of the material (figure 2). For that, we use the classic definition [3]

$$\%tunability = \frac{\epsilon'(0) - \epsilon'(E_{bias})}{\epsilon'(0)} \times 100 \quad (1)$$

where $\epsilon'(0)$ and $\epsilon'(E_{bias})$ are the permittivity without and under the bias electric field E_{bias} . The samples present here a tunability of 42.1 %.

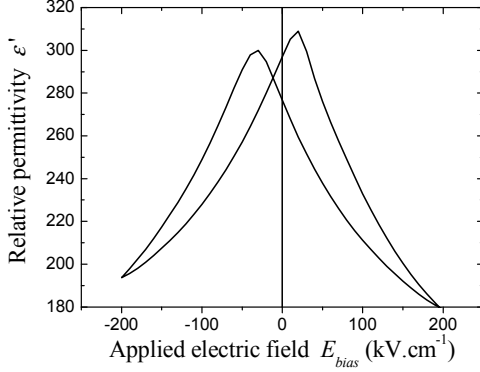


Figure 2. Butterfly ϵ - E loops of PZT 43/57 at 300 K.

The capacitance C and the dielectric loss factor ($\tan \delta$) were measured using an impedance meter (*Agilent 4294A*) with a low ac field E_{exc} on 100 Hz - 100 MHz domain frequencies. The real and imaginary parts of the permittivity (ϵ' and ϵ'' respectively) are calculated with

$$\epsilon' = \frac{C}{\epsilon_0} \frac{e}{S} \quad \text{and} \quad \epsilon'' = \tan \delta \cdot \epsilon' \quad (2)$$

ϵ_0 is the permittivity of free space.

III. RESULTS AND DISCUSSIONS

A first series of measurements allows us to obtain the real part ϵ' and imaginary part ϵ'' of the permittivity as a function of the frequency at different temperatures. Results are reported on figure 3. A relaxation is observed on the frequency domain studied and is attributed to the domain wall movements [4]. Under the influence of the electric field, domain walls can either vibrate around their equilibrium position (pinning centers) or jump from a center to another. The relaxation time τ is defined by $\tau = 1/\omega_0$ where ω_0 is the pulsation for which $\epsilon''(\omega)$ is maximum (or for which $\epsilon'(\omega)$ admits an inflection point). His relaxation time increases with temperature and the values of ϵ_s and ϵ_∞ ($\epsilon_s = \lim_{\omega \rightarrow 0} \epsilon'(\omega)$, $\epsilon_\infty = \lim_{\omega \rightarrow \infty} \epsilon'(\omega)$) also increase. At low frequencies, diffusion process appears for the highest values of T . Generally, one can write [5]

$$\epsilon'(\omega) = \epsilon_\infty + \Delta\epsilon \int_0^\infty \frac{g(\tau)}{1 + \omega^2 \tau^2} d\tau \quad (3)$$

$$\epsilon''(\omega) = \Delta\epsilon \int_0^\infty \frac{g(\tau) \omega \tau}{1 + \omega^2 \tau^2} d\tau$$

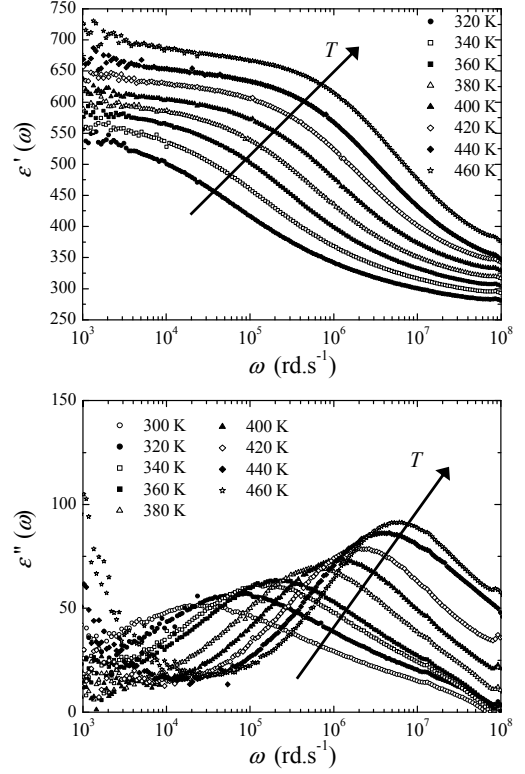


Figure 3. Evolution of ϵ' (top) and of ϵ'' (bottom) as a function of the angular frequency ω and of the temperature T .

where $\Delta\epsilon = \epsilon_s - \epsilon_\infty$. $g(\tau)$ is the distribution of the relaxation time which is specific to studied relaxation. Generally, it is impossible to obtain $g(\tau)$ only from the knowledge of $\epsilon'(\omega)$ and $\epsilon''(\omega)$.

Figure 4 the Argand diagram, one realizes that data are well approximated by a Cole-Cole arc. In the Cole-Cole theory, the complex permittivity is done by ($p = \omega\tau$) [6]

$$\epsilon^*(\omega) = \epsilon_\infty + \frac{\Delta\epsilon}{1 + (ip)^{1-\beta}} \quad (4)$$

with β a dispersion parameter which accounts for the width of the distribution of the relaxation time ($\beta = 0$ correspond to a single relaxation time, i.e. Debye formalism).

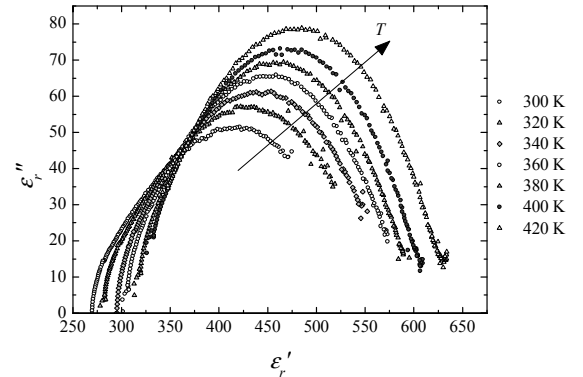


Figure 4. Evolution of the Argand diagram for several temperatures. For a better visibility of the figure, scales are not identical on the two axes.

This can be also expressed by

$$\begin{aligned} \varepsilon'(\omega) &= \varepsilon_\infty + \Delta\varepsilon \frac{1 + p^{1-\beta} \sin(\beta\pi/2)}{1 + p^{2(1-\beta)} + 2p^{1-\beta} \sin(\beta\pi/2)} \\ \varepsilon''(\omega) &= \Delta\varepsilon \frac{p^{1-\beta} \cos(\beta\pi/2)}{1 + p^{2(1-\beta)} + 2p^{1-\beta} \sin(\beta\pi/2)}. \end{aligned} \quad (5)$$

Parameters ε_∞ , $\Delta\varepsilon$, τ and β are determined by fitting curves of figure 3 with equations (5). We found that ε_∞ follows a Curie-Weiss law ($T_C = 770$ K) while $\Delta\varepsilon$ does not depend on the temperature (figure 5). Thus ε_s also follows a Curie-Weiss law as awaited for ferroelectric materials.

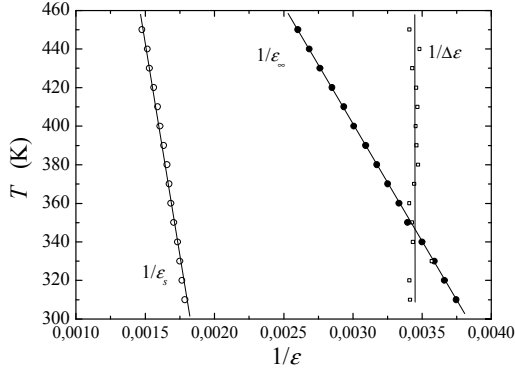


Figure 5. Variation of ε_s , ε_∞ and $\Delta\varepsilon$ with temperature.

As shown on figure 6, the relaxation time τ obeys to an Arrhenius law which corresponds to a thermally activated process

$$\tau = \tau_0 \exp\left(\frac{E_a}{k_B T}\right). \quad (6)$$

E_a is the activation energy and equals here to 0.38 eV. We found also $\tau_0 = 12.6$ ps and $1/\tau_0$ well corresponds to the phonon vibration frequency. k_B is the Boltzmann constant.

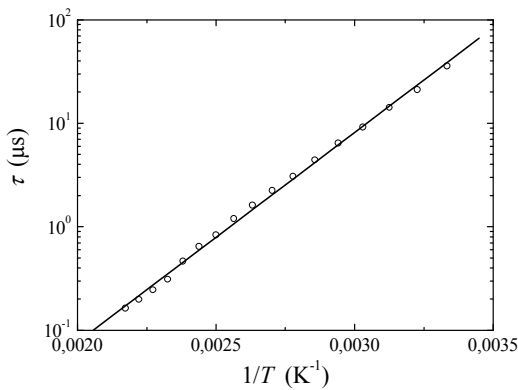


Figure 6. Variation of τ as a function of temperature.

On the temperature domain studied here, β seems to have a linear dependence with temperature (figure 7), decreasing when T increases. However, it is difficult to interpret this result because β has not a direct physical signification.

As already mentioned, the movement of domain walls under the influence of a low ac electric field E_{exc} can corresponds either to a vibration around the equilibrium position, or to a jump towards another equilibrium position. For the permittivity, that results in the hyperbolic law [7]

$$\varepsilon = \varepsilon_{bulk} + \sqrt{\varepsilon_{rev}^2 + \varepsilon_{irrev}^2} = \varepsilon_{bulk} + \sqrt{\varepsilon_{rev}^2 + \alpha^2 E_{exc}^2}. \quad (7)$$

ε_{bulk} is the permittivity due to intrinsic lattice contributions, ε_{rev} the dielectric constant related to domain walls vibrations which correspond to a reversible process [8]. The parameter α represents domain walls pinning and is related to an irreversible modification of the local polarization [9]. Both parameters depend on the crystal structure, but α also reflects the presence of impurities, dopants or defects [8]. This law is only valid if $E_{exc} < E_C/2$ ($= 45$ kV·cm⁻¹ here) [7-8].

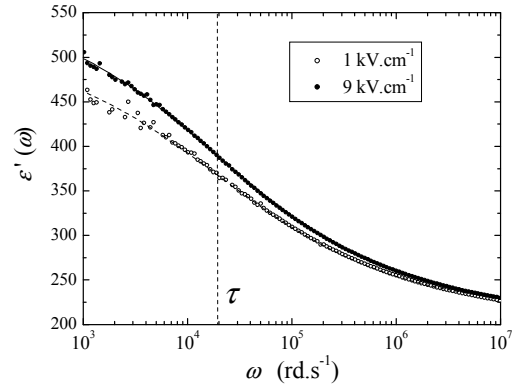


Figure 7. Variation of ε' as a function of ω for two values of E_{exc} .

In a second series, the temperature is fixed at 300 K and ε' and ε'' are measured for two values of E_{exc} , 1 kV·cm⁻¹ and 9 kV·cm⁻¹ (figure 7). The field effect is only perceptible at low frequencies and in particular, fits show that ε_∞ is independent of E_{exc} . Consequently, for $\omega \gg 1/\tau$, domain walls do not jump any more.

We have also measured the variations of ε' and ε'' as the function of field E_{exc} at various frequencies (1, 10, 100 and 1000 kHz) and plot the Argand diagrams for the different contributions to the permittivity (bulk, reversible and irreversible). Results are reported on figure 8.

It is noticed that each contribution to the permittivity is described by a Cole-Cole law with a very different dispersion parameter β . On a Argand diagram, the relaxation time is obtained by the frequency which corresponds to the maximum of ε'' . The values of τ estimated by this way for each contribution are practically the same excepted for the irreversible contribution. In this last case, a wall jumping from a site to another is difficult to realize and the relaxation time is very large. In both other cases, there are always some dipole vibrations, either in the domain wall or in the lattice. Thus, the relaxation times of bulk and reversible contributions are similar.

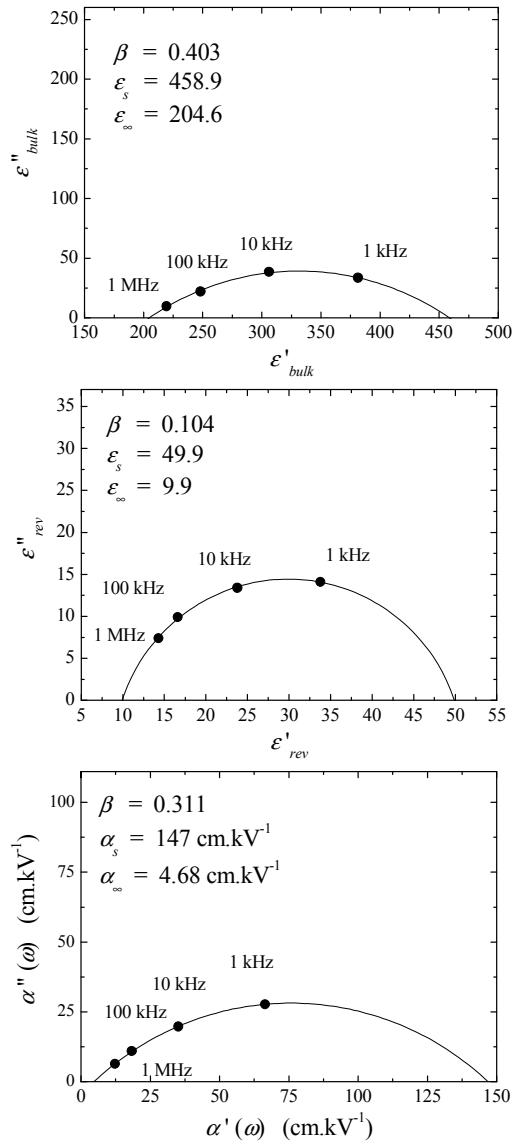


Figure 8. Argand diagram for the bulk (top), the reversible (middle) and irreversible (bottom) contributions.

To finish, we plot the tunability of the sample as a function of E_{exc} (figure 9). It seems interesting to work with the greatest amplitude of E_{exc} . However, losses also increase with the field amplitude [4]. We can then define a figure of merit by

$$F.O.M. = \frac{\text{Tunability}}{\tan \delta_{\max}}. \quad (8)$$

On figure 9, we see that the $F.O.M.$ decrease when the field amplitude E_{exc} increases. The losses increase more quickly than the real permittivity. So, to have a better compromise between the tunability and the losses, it thus appears preferable to work with an electric field of low amplitude.

IV. CONCLUSIONS

The study of PZT 43/57 shows that the permittivity is correctly described by the Cole-Cole model. The relaxation time is done by the Arrhenius law corresponding to a thermally

activated process with an activation energy equals to 0.38 eV. The hyperbolic law shows that permittivity has three different contributions. The contribution associated with the domain wall jumps depends on the amplitude of the applied ac electric field. Thus, for devices including ferroelectric thin films, it is important to control this parameter. The values of the permittivity and tenability are significantly influences by the electric field. Because of the dielectric losses which also grow with the field, it is advised to use a reconfigurable device with a field amplitude the weakest possible.

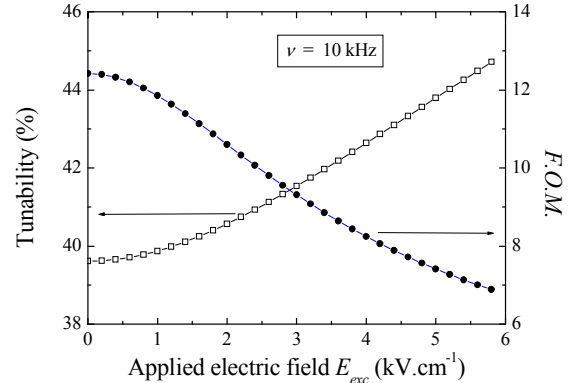


Figure 9. Tunability (Top) and Figure Of Merit (bottom) as a function of E_{exc} .

REFERENCES

- [1] N. V. Giridharan, S. Madeswaran, and R. Jayavel, "Structural, morphology and electrical studies on ferroelectric bismuth titanate thin films prepared by sol-gel technique," *Journal of Crystal Growth*, vol. 237-239, pp. 468-472, 2002.
- [2] H.-Y. Tian, W.-G. Luo, X.-H. Pu, X.-Y. He, P.-S. Qiu, and A.-L. Ding, "Synthesis and dielectric characteristic of $Ba_{1-x}Sr_xTiO_3$ thin films-based strontium-barium alloxides derivatives," *Materials Chemistry and Physics*, vol. 69, pp. 166-71, 2001.
- [3] H. N. Al-Shareef, D. Dimos, M. V. Raymond, R. W. Schwartz, and C. H. Mueller, "Tunability and calculation of the dielectric constant of capacitor structures with interdigital electrodes," *Journal of Electroceramics*, vol. 1, pp. 145-153, 1997.
- [4] C. Borderon, "Développement et étude des matériaux ferroélectriques accordables en vue d'une application pour les antennes intelligentes" PhD Thesis, University of Nantes, 2008.
- [5] I. Bunget, M. Popescu, *Physics of solids dielectrics*, Elsevier, 1984, pp.282-291.
- [6] K.S. Cole, R.H. Cole, "Dispersion and absorption in dielectrics. I-Alternating current characteristics", *Journal of Chemical Physics*, vol. 9, pp. 341-351, 1941.
- [7] C. Borderon, R. Renoud, M. Ragheb, and H. W. Gundel, "Description of the low field nonlinear dielectric properties of ferroelectric and multiferroics materials," *Applied Physics Letters*, unpublished.
- [8] O. Boser, "Statistical theory of hysteresis in ferroelectric materials," *Journal of Applied Physics*, vol. 62, pp. 1344-1348, 1987.
- [9] N. B. Gharb and S. Trolrier-McKinstry, "Dielectric nonlinearity of $Pb(Yb_{1/2}Nb_{1/2})O_3$ - $PbTiO_3$ thin films with $\{100\}$ and $\{111\}$ crystallographic orientation," *Journal of Applied Physics*, vol. 97, pp. 64106, 2005.